An Aerodynamic Analysis of Several Hypersonic Research Airplane Concepts from $M = 0.2$ to 6.0

Jim A. Penland,* James L. Dillon,† and Jimmy L. Pittman†
NASA Langley Research Center, Hampton, Va.

Several conceptual hypersonic research airplanes, designed within the constraints of a B-52 launch aircraft, were studied experimentally and analytically at Mach numbers from 0.2 to 6.0. Vehicles built to these criteria for Mach 6 cruise were shown to be feasible. The integrated scramjet engine drag approached that of a flat plate normal to the flow at subsonic speeds and appeared to be relatively constant with Reynolds number. The variable geometry airfoil used previously to improve directional stability was shown to be equally adaptable to the improvement of longitudinal stability. The vortex lattice theory gave good subsonic predictions of lift, drag due to lift, and pitching moments. It was found that wind tunnel tests must be relied upon for the drag at zero lift, trim, static margins, and lateral-directional stability. The Gentry Hypersonic Arbitrary Body Program gave good predictions of the trends of lift, drag, and pitching moments with angle-of-attack at Mach numbers above 3, but the magnitudes were not consistently predicted. No currently available theory or program gave accurate predictions of directional stability or dihedral effects at hypersonic speeds.

Nomenclature

AR	= aspect ratio, b^2/S
b	= wing span
C_D	= drag coefficient, drag/qb^2
C_F	= skin friction coefficient
C_L	= lift coefficient, lift/qb^2
C_m	= pitching moment coefficient, pitch/$qb^2\ell$
C_l	= rolling moment coefficient, rolling moment/qb^3
C_{l_β}	= rate of change of C_l with sideslip angle, per deg
$C_{l_{\delta h}}$	= rate of change of C_l with roll control angle, per deg
$C_{l_{\delta V}}$	= rate of change of C_l with yaw control angle, per deg
C_{m_α}	= rate of change of C_m with angle-of-attack, per deg
C_n	= yawing moment coefficient, yawing moment/qb^3
C_{n_β}	= rate of change of C_n with sideslip angle, per deg
$C_{n_{\delta h}}$	= rate of change of C_n with roll control angle, per deg
$C_{n_{\delta V}}$	= rate of change of C_n with yaw control angle, per deg
C_Y	= side force coefficient, side force/qb^2
ℓ	= fuselage length
L/D	= lift-to-drag ratio
M	= freestream Mach number
q	= freestream dynamic pressure
R_L	= Reynolds number based on fuselage length
S	= wing planform area
α	= angle-of-attack
β	= angle of sideslip
$\Lambda_{c/4}$	= sweep of quarter chord

Subscripts

b	= base
max	= maximum
min	= minimum
0	= condition at zero lift
S.J.	= scramjet
V.L.	= vortex lattice
δh	= differential elevon deflection for roll control
δV	= vertical tail deflection for yaw control

Presented as Paper 78-150 at the AIAA 16th Aerospace Sciences Meeting, Huntsville, Ala., Jan 16-18, 1978; submitted Feb. 15, 1978; revision received May 26, 1978.

Index categories: Configuration Design; Analytical and Numerical Methods; Airbreathing Propulsion.

*Aero-Space Technologist, Hypersonic Aerodynamics Branch, High-Speed Aerodynamics Division. Member AIAA.

†Aero-Space Technologist, Hypersonic Aerodynamics Branch, High-Speed Aerodynamics Division.

Introduction

RESEARCH airplanes have been used extensively in exploring high-speed flight regimes since the end of World War II. These airplanes have ranged from the X-1 which first achieved Mach 1 in 1947 to the X-15 which reached Mach 6.7 in 1967. The X-15 program ended shortly thereafter, and during the past ten years no manned aircraft has explored the speed region beyond $M = 3$.[1] Since the termination of the X-15, NASA and the USAF have conducted a number of studies to define a new research aircraft to supplement ground-based experimental facilities and to provide verification and improvement of present high-speed flight technology. Recent studies have included the National Hypersonic Flight Research Facility (NHFRF), an air-launched rocket-powered vehicle capable of speeds up to $M = 8$ with provisions for conducting flight research for a wide variety of hypersonic technologies including airbreathing propulsion, airframe structures, weapons, and liquid-hydrogen fuel systems.

Figure 1 shows an early concept mated to the B-52 launch aircraft. A B-52 launch aircraft restricts the maximum span of the research vehicle to 24 ft, the height to 9 ft to provide ground clearance, and the weight to 70,000 lb. The length and empennage design must also be made with consideration for the B-52 engine exhaust and its possible deleterious effects on the research airplane due to buffeting and vibration.

The early research airplane concept shown in Fig. 1 has several features common to all of the present configurations. These include a voluminous fuselage of about 2730 ft^3 to house the pilot, a 10-ft-long experiments bay, various

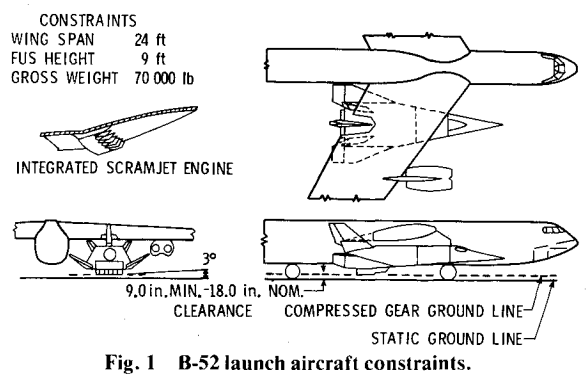

Fig. 1 B-52 launch aircraft constraints.

systems, and fuel for the rocket booster engine. Large vertical tail surfaces are needed to maintain directional stability up to the hypersonic cruise speeds of $M=6$ to 8. The bottom-mounted integrated scramjet engine concept (see inset) is a primary experiment incorporated on all configurations reported in this paper and utilizes the complete lower surface of the aircraft fuselage. The forebody provides precompression of the air; the engine modules contain additional compression surfaces, fuel ejector struts, and combustors, followed by the exhaust nozzle which expands to the base of the vehicle. This nozzle is important to the performance of hypersonic aircraft because it provides up to one-half of the cruise thrust at $M=6$. Its contribution to net thrust is a function of not only the expansion angle downstream of the engine nodules but also the length of the nozzle. This nozzle angle and length can affect subsonic landing performance and will be discussed subsequently.

The purpose of this paper is to present some of the important aerodynamic performance and stability and control characteristics for research aircraft that meet the geometric restrictions imposed by an air launch from a B-52. Vehicle flight attitude, shape, and Mach number are considered and wind tunnel data are compared with available analytical techniques. Since the wing span was common to all concepts, the square of the span (b^2) was used instead of wing reference area in nondimensional aerodynamic coefficients.

Models, Apparatus, and Tests

The experimental data presented in the present paper were measured on metal models using six component strain gage balances in LRC wind tunnels. These models were fabricated with interchangeable parts and adjustable control surfaces to make possible limited parametric studies as well as the determination of trim and control characteristics.

Tests were conducted in the following LRC facilities at the Mach numbers and Reynolds number based on model length shown: the low turbulence pressure tunnel at $M=0.2$ through a Reynolds number range of about 2 to 30×10^6; the 8-ft-transonic pressure tunnel at $M=0.8$ to 1.2 at a Reynolds number of about 6×10^6; the unitary plan wind tunnel at $M=1.5$ to 2.86 at a Reynolds number of about 4×10^6; and the 20-in. hypersonic tunnel at $M=6.0$ and a Reynolds number of about 14×10^6.

All tests were made with fixed transition[2] except those at $M=0.2$ with variable Reynolds number and tests at $M=6$ which were made with free transition. Base pressures were measured for all tests, and drag coefficients were corrected to freestream static pressure on the base for all Mach numbers greater than 0.2.

Results and Discussion

Subsonic Aerodynamics

Subsonic Performance

The maximum lift-to-drag ratio is one measure of the subsonic performance and landing qualities of a vehicle. Figure 2 presents a low-speed component buildup of this early concept (A) and the resulting decrease in $(L/D)_{max}$ with the addition of each component. The single largest loss in efficiency was the addition of the vertical tails which were required for directional stability. The side vertical tails were toed-in for effectiveness at hypersonic speeds and this toe-in alone accounted for about one-half unit decrease in subsonic $(L/D)_{max}$. The use of variable geometry for toe-in control could therefore be beneficial in minimizing losses in one speed range due to the required component attitudes for another speed range. The addition of the scramjet engine, the deployment of the landing gear, and trim drag all resulted in a very low $(L/D)_{max}$. It was concluded[3] that additional pilot aids would be required to facilitate the landings of vehicles having L/D ratios of 3 or less. Since aircraft do not necessarily land at angles of attack for $(L/D)_{max}$, a cushion or safety factor of one or two units of L/D would also be desirable. It was therefore concluded that the performance of this early concept was unsatisfactory and that improvements were in order.

The results of an effort to improve the performance of concept (A) are shown in Fig. 3. An increase in $(L/D)_{max}$ occurred when the scramjet external exhaust nozzle deflection angle was decreased by the deflection of a bottom flap. This incremental improvement occurred even though the base area increased by almost 30%, and will be discussed in more detail subsequently. It was estimated that the substitution of a single center vertical tail, having a tail volume equivalent to that of the original three vertical tails, would improve the $(L/D)_{max}$ due to decreased interference effects and the greater span and aspect ratio. Tests were conducted on the enlarged single vertical tail in combination with a 50% decrease in the base area made possible by boattailing. This combination gave more than a unit increase in $(L/D)_{max}$ relative to the early concept. An estimate was made showing that $(L/D)_{max}$ could be increased by about two units if the entire base area was eliminated on the basic clean configuration. Such decreases in base area are impractical, particularly for a rocket-boosted craft, but these decreases emphasize the serious losses due to base drag at subsonic speeds. Although significant gains in $(L/D)_{max}$ may be made by boattailing a given configuration, care must be taken to decrease the cross section gradually to assure shallow convergence angles and minimize the possibility of flow separation. These improvements in the performance of the early concept have been significant, but the resulting $(L/D)_{max}$ with scramjet installed and landing gear deployed is still only about 3.3, a value which is only marginally acceptable and allows no room for vehicle growth. Other methods of increasing the lift and decreasing the drag were therefore required. The basic lifting body configuration

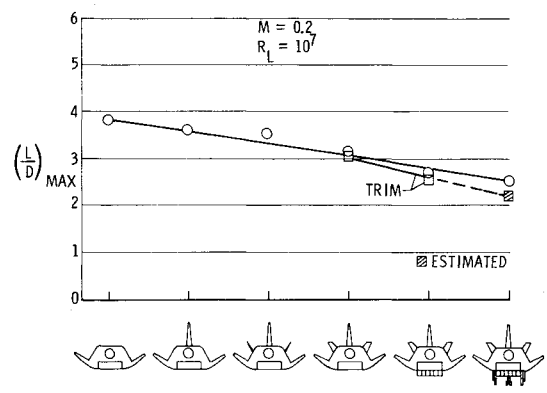

Fig. 2 Decrease of L/D_{max} with component buildup for early lifting body concept A.

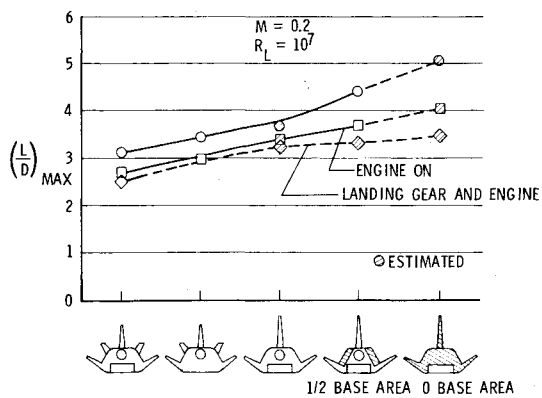

Fig. 3 Increase of L/D_{max} by variation in design for early lifting body concept A.

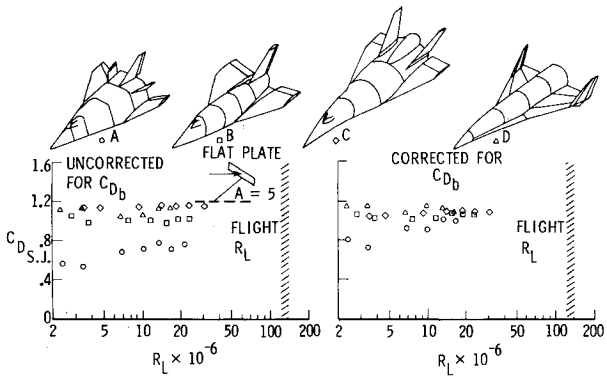

Fig. 4 Variation of scramjet engine drag with Reynolds number, $M = 0.2$.

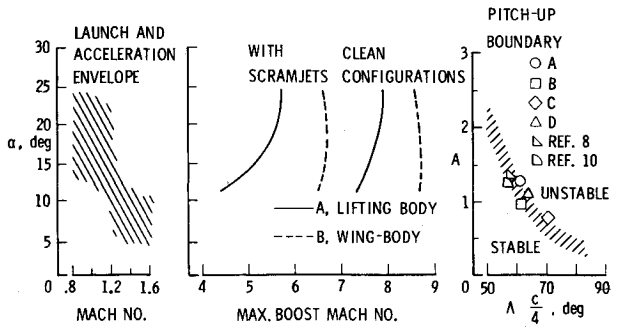

Fig. 5 Effect of vehicle pitchup on maximum boost Mach number.

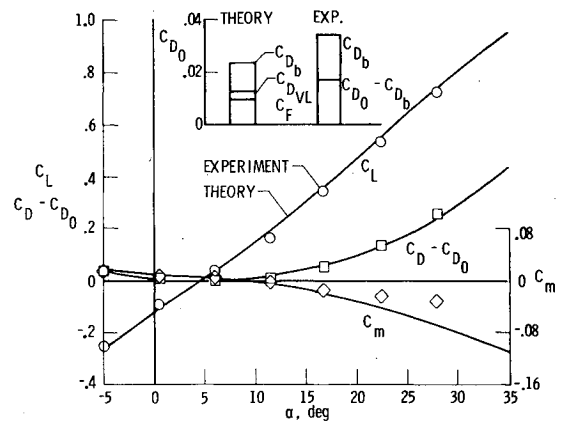

Fig. 6 Comparison of theory and experiment for configuration A, without vertical tails or engine, $M = 0.2$, $R_L = 10^7$.

was redesigned to provide more efficient lifting surfaces by stretching the fuselage and exposing more wing, and by decreasing base drag through minimizing base area. This intermediate design is identified herein as the wing-body concept (B). Another avenue of study was to investigate the drag attributable to the engine installation.

Scramjet Engine Drag

The variation of scramjet engine drag with Reynolds number at a constant Mach number of 0.2 is presented in Fig. 4. Shown in outline form are the early lifting body concept designated (A), the wing-body concept (B), the preliminary design concept (C),[4] and a reference concept (D).[5,6] Concepts A, B, and C will be discussed at length in the remainder of this paper.

Subsonic scramjet engine drag on these four different models is presented both uncorrected for base pressure, and with the base pressure corrected to freestream static pressure. The drag coefficients are referenced to the engine inlet (frontal) area and were obtained at $C_L = 0$. The engine on each model consisted of six modules except the engine on model C which consisted of eight modules. Details of the flight engine design and a discussion of its integration with the airframe may be found in Refs 7-9. The model test engines were built with the correct external leading edge sweep, wedge angles, and scale areas, and except for model D the correct internal contraction ratio, but with only a single strut having a scale cross-sectional area equal to the three fuel struts of the flight design. Model D had no simulated fuel strut. This method of simulating geometric contraction was found to be satisfactory.[9]

It may be seen that the drag coefficients of all engines tested approached that of a flat plate with aspect ratio 5, normal to the flow. The width/height ratio for the model engines was approximately 5. These high engine drag coefficients on the 1/30-scale models of the present tests were validated on 1/10-scale model tests.[9] The same instrumentation was used for measuring the drag of each of the present configurations, and therefore the accuracy of the data would be expected to improve with increasing Reynolds number, which accounts for the greater scatter of data points at the lower Reynolds number. The data which have been corrected for base pressure appear to have less scatter generally than those which are shown uncorrected and indicate the effect of engine installation on base pressure. By either method of presentation, an extrapolation to flight Reynolds number would yield a drag coefficient of about 1.15. It may therefore be concluded that within the scatter of wind tunnel data the drag coefficient of this integrated scramjet engine concept is relatively constant with Reynolds number at subsonic speeds (and independent of configuration type).

High-Angle-of-Attack Stability

Flight profiles have been established through computerized trajectory analysis using the data from extensive wind tunnel tests on the lifting body (A) and the wing-body (B) concepts. The results of these studies showed that, due to the high transonic drag of the concepts and the associated high fuel consumption, the most efficient flight trajectory was one that traversed the transonic region as rapidly as possible.

Figure 5 presents a summary of these trajectory studies and the basis for requiring high-angle-of-attack subsonic longitudinal stability. This figure shows an angle-of-attack history of launch and acceleration through the transonic and low supersonic Mach number range, the effect of pullup angle of attack on the maximum boost Mach number, and a review of subsonic pitchup as a function of vehicle geometry. The angle-of-attack history shows the relatively high angle-of-attack required after launch and the decrease to relatively low angles for acceleration once a high flight path angle trajectory has been established. Low angles-of-attack are flown through the rocket-boosted acceleration to cruise Mach number and deceleration back to subsonic speed where again the high angles-of-attack are required for landing.

The effect of the pullup angle-of-attack on the attainment of maximum boost Mach number is illustrated for the concepts A and B. The low-efficiency lifting body concept A shows considerable sensitivity to the pullup angle-of-attack. A pullup of only 11 deg would yield a maximum boost Mach number for the case with scramjet installed of only 4.5 whereas a pullup to 23 deg yields a boost Mach number of about 5.8. The more efficient wing-body concept (B) is less sensitive to pullup angle-of-attack and appears to achieve its maximum boost Mach number at about $\alpha = 15$ deg. The sensitivity to pullup angle-of-attack is greatly decreased for the scramjet-off, clean configurations. Concept B, however, is shown to achieve about one full Mach number higher speed than concept A.

An empirical pitchup boundary for simple wings is shown as a function of aspect ratio and sweep of the quarter chord line.[10] Superimposed on this plot are the present research airplane concepts and two other reference configurations. It is

not known if the pitchup criteria for simple wings in subsonic flow is indicative of what may be expected of complete configurations having similar aspect ratios and wing sweeps. However, models B and that of Ref. 11 exhibited no instability at angles-of-attack up to 35 and 30 deg respectively, models A and D became neutrally stable at $\alpha = 28$ deg and models C and that of Ref. 8 showed unstable tendencies at $\alpha = 30$ and 25 deg, respectively. Limited high-angle-of-attack data preclude firm conclusions on the present concepts. However, these studies indicate that the low aspect ratio due to the span limitation imposed by the B-52 launch aircraft and the high wing sweep needed to minimize hypersonic aerodynamic heating and wave drag drive the present concepts toward a region of proven longitudinal instability for simple wings. Due to the maneuvers required of the research airplane, it is mandatory that the pitchup characteristics be known early in the design phase of development.

Subsonic Experiment and Theory

The application of incompressible wing theory to complete configurations has produced some useful results. Figures 6–8 present a comparison of experimental data and the theory of Ref. 12 at $M = 0.20$ for configurations consisting of only the fuselage and wing of each of the study concepts, A, B, and C. No vertical tails or engine modules were included in these calculations. The data have been corrected to the condition of freestream static pressure acting on the fuselage base. The theory represents the configuration by a planar vortex lattice and accounts for wing leading edge and wing tip flow separation through the use of suction analogy.[13] About 125 elemental panels were used to describe the fuselage and wing for each concept. A discussion on the effect of elemental panel density for configurations of this type can be found in Ref. 14.

Overall agreement between theory and experiment for lift (C_L), drag due to lift ($C_D - C_{D,0}$), and pitching moment (C_m) is good with large differences occurring only at high angles-of-attack. The data were plotted against angle-of-attack rather than C_L so that one parameter is independent of the solution accuracy. Also shown on each figure is an estimated $C_{D,0}$ determined by the methods of Ref. 15, and the vortex lattice theory. From Ref. 15 an estimate of the skin friction drag, the form drag, and the base drag were obtained. The vortex lattice theory, which is inviscid, predicts the induced drag. At $C_L = 0$, there is an induced-drag component $C_{D_{VL}}$ of $C_{D,0}$ which is a result of the spanwise variation of the mean camber surfaces of the fuselage and wing. This induced-drag component of $C_{D,0}$ was subtracted from the vortex lattice induced-drag prediction for the comparison with experiment through the angle-of-attack range. An estimate of the small increment of grit drag was not included in the $C_{D,0}$ prediction. The accuracy of the estimates of $C_{D,0}$ varied considerably between configurations.

From this comparison of theory and experiment on three configurations it may be concluded that good predictions of lift, drag due to lift, and pitching moment can be made using the vortex lattice theory. Current methods of predicting drag at zero lift are undependable and wind tunnel tests are required for accurate $C_{D,0}$ values and trim characteristics.

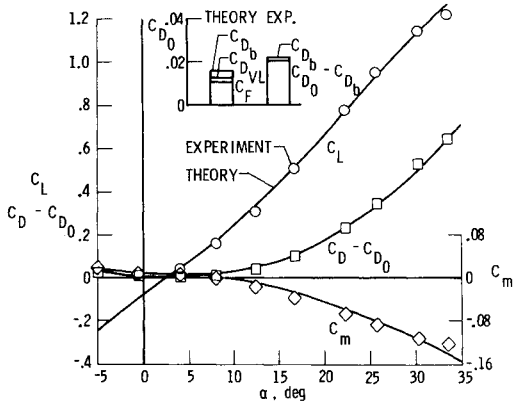

Fig. 7 Comparison of theory and experiment for configuration B, without vertical tails or engine, $M = 0.2$, $R_L = 14 \times 10^6$.

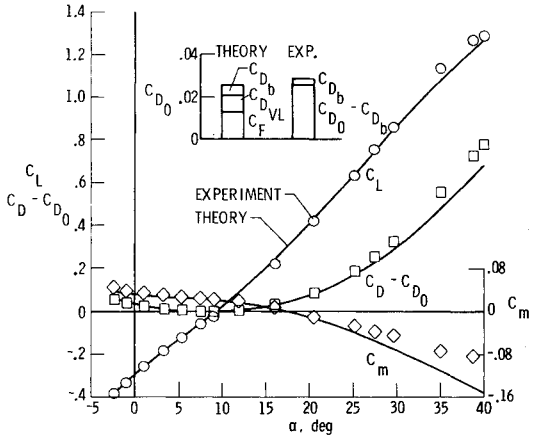

Fig. 8 Comparison of theory and experiment for configuration C, without vertical tails or engine, $M = 0.2$, $R_L = 16 \times 10^6$.

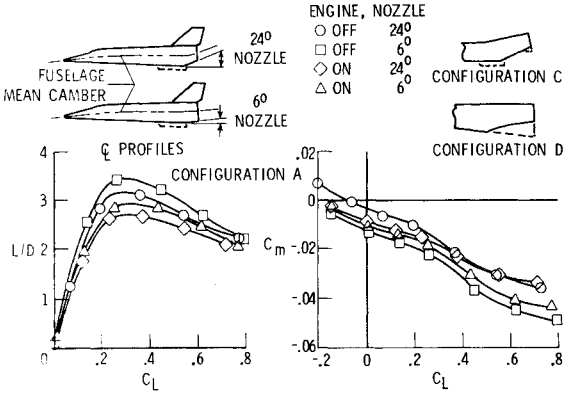

Fig. 9 Subsonic effects of nozzle geometry variation, $M = 0.2$, $R_L = 10^7$.

Subsonic Effects of Nozzle Geometry Variations

During the analysis of test data on the present design concepts of A, C, and D a similar phenomenon was observed on each configuration in the relation of the maximum lift-to-drag ratio to geometric variations made to each scramjet nozzle. In each case the L/D_{max} was observed to improve when the nozzle was either partially or fully faired in. Figure 9 shows the variation in L/D and C_m with angle-of-attack for model A with and without the model scramjet engine installed. The nozzle expansion angle was reduced from 24 deg to 6 deg by a bottom flap deflection and was accompanied by a 10% increase in L/D_{max}, despite the fact that the base area was increased with flap deflection. The base pressure coefficient remained essentially constant within the accuracy of measurement for the nozzle geometry variations. The positive flap deflection also produced a more nose down pitching moment as would be expected for a normal control. The inset line drawings show the nozzle alterations tested on models C and D which showed similar improvements in performance. These trends are thought to be due in part to variations in separation in the vicinity of the nozzle.

An analytic study was initiated to gain a better understanding of the experimental trends. The original input for the vortex lattice calculations was altered to account for the variations in the mean camber surface of the body due to the bottom nozzle flap deflection. The results showed that the

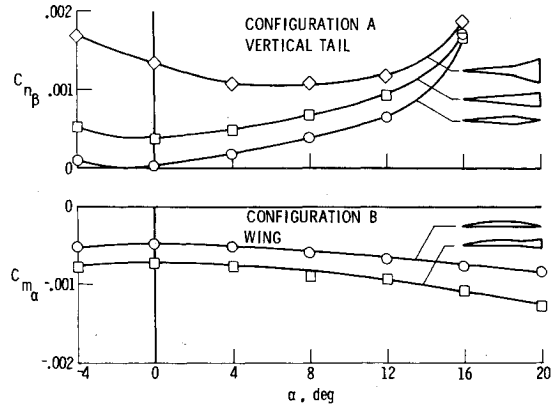

Fig. 10 Static stability improvement with airfoil section variation, $M=6.0$.

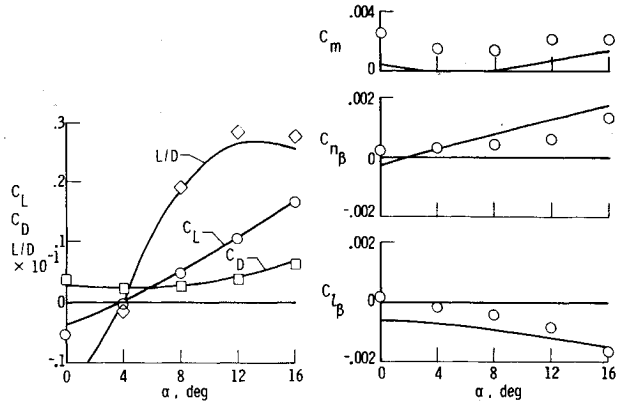

Fig. 11 Comparison of theory and experiment for configuration A, without engine, $M=6.0$, $R_L=13\times10^6$.

straightening of the reflexed camber line increased the lift and slightly reduced the drag due to lift. Therefore, if the $C_{D,0}$ was assumed to remain constant, the L/D would necessarily increase. The calculated pitching moment curves also showed a nose-down increment of pitch. This suggests that the gain in L/D was due not only to reduced separation but to an increase in pressure in the vicinity of the nozzle (decrease in negative lift) which in turn decreased the drag due to lift and, because the nozzle was behind the center of gravity, produced a nose-down pitching moment.

Hypersonic Aerodynamics

The discussion has thus far dealt primarily with subsonic experimental and theoretical aerodynamics. The next few figures present a similar review of hypersonic studies at $M=6$.

Hypersonic Stability and Airfoil Sections

The concept of using wedge-shaped airfoils to enhance directional stability at hypersonic speeds was originated during the X-15 wind tunnel test program[16] and was used on the full-scale aircraft. A similar variable geometry vertical tail is presently installed on the space shuttle to not only increase the stabilizing effectiveness at hypersonic speeds but to also act as speed brakes with further trailing edge flare.

The results of wind tunnel tests at $M=6$ are presented in Fig. 10 which shows the improvement of directional stability ($C_{n\beta}$) with increased rudder flare on the center vertical tail of the lifting body model A. Similarly, an improvement of longitudinal stability was observed with flared elevons on the wing-body model B. the present tests consisted of a ±5 deg flare on the model B elevons, and the data show up to a 50% increase in the slope of the pitching moment with angle-of-attack ($C_{m\alpha}$), and an increase in the static margin of approximately 1.8% body length. It appears that the variable

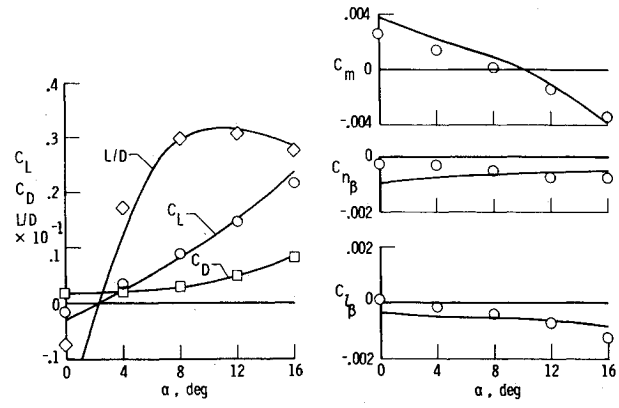

Fig. 12 Comparison of theory and experiment for configuration B, without engine, $M=6.0$, $R_L=14\times10^6$.

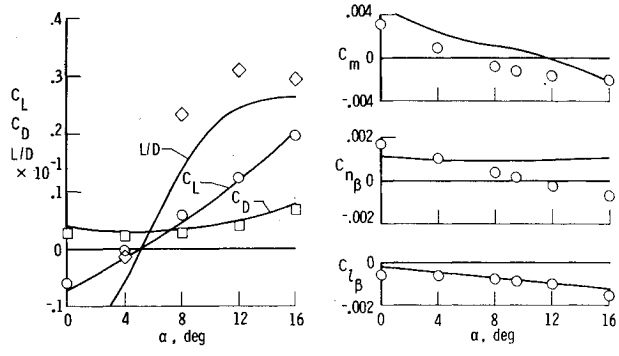

Fig. 13 Comparison of theory and experiment for configuration C, without engine, $M=6.0$, $R_L=16\times10^6$.

geometry airfoil, invaluable as a device to improve the directional stability of aircraft at hypersonic speeds, may be equally applied to the wing airfoil of an all-wing aircraft in the form of flared elevons to improve the longitudinal stability. Either application is suited for use as a speed brake across the speed range.

Hypersonic Experiment and Theory

The ability to predict the performance and the longitudinal, lateral, and directional stability and control of complete aircraft configurations at hypersonic speeds has progressed little in the past 15 years. The Master Dimensions Program[17] of the early 1960's made possible the calculation of the aerodynamics of complete configurations using the Newtonian theory, and later program modifications made possible the use of tangent-wedge or tangent-cone pressure distributions to replace the modified Newtonian concept. In the late 1960's the Gentry Hypersonic Arbitrary Body Program[18] made possible the use of combined inviscid and viscid calculations, a variety of possible aerodynamic theories, and straightforward computer inputs. Additional input simplification has been achieved by using the methods of Ref. 19.

The purpose of this section is to present a comparison (Figs. 11-13) of the experimental aerodynamics of configurations A, B, and C at $M=6.0$ and calculations made using the Gentry Arbitrary Body Program. The tangent-cone theory was used for compression surface pressure calculations on the fuselage of each configuration and the tangent-wedge theory for the wing and vertical tail surfaces. The Prandtl-Meyer expansion theory was utilized to calculate the pressures in expansion regions on all components. Turbulent skin friction was calculated using the Spalding-Chi method.

A study of Figs. 11-13 shows a consistent prediction of the trends of the performance parameters, C_L, C_D, and L/D with angle-of-attack and of the longitudinal stability parameter C_m. The angle-of-attack for $C_L=0$ was predicted within $\alpha=1$

deg for all configurations. However, the angle-of-attack for trim ($C_m = 0$) was in error as much as $\alpha = 6$ deg, thereby precluding even reasonably accurate trim calculations. The neutral to unstable trend of the pitching moment curve for configuration A (Fig. 11) was predicted; however, the level of C_m was underpredicted for configuration A and overpredicted for configurations B and C (Figs. 12 and 13). Because of the relatively accurate prediction of the trends of C_m and C_L, particularly the local slopes with angle-of-attack, an examination of only the calculated values of C_L, C_m, and the slope $\partial C_m/\partial C_L$ (the static margin) without benefit of experimental data could lead to a false or distorted conclusion regarding the pitch and trim of a given vehicle. Failure of the programs to accurately predict the pitching moments is due to the simplified nature of the tangent-cone and tangent-wedge pressure prediction theories which do not take into account the history of the flow along the surface or the mutual interference between components. It should be noted in this regard that using shock expansion theory on the wings of these particular configurations, instead of the tangent-wedge theory, does not improve the C_m predictions. The lift-drag ratio L/D was well predicted for configurations A and B but underpredicted for configuration C due mainly to an overprediction of drag. It may be concluded that at $M = 6$, the Gentry Program accurately predicts the trends, including the local slopes of C_L, C_D, and C_m with angle-of-attack for this class of vehicle, but the level of the values of C_m, C_D, and L/D and the angles of attack for $C_L = 0$ and $C_m = 0$ are not consistently predicted.

The prediction of the very important parameters of directional stability C_{n_β} and dihedral effect C_{l_β} by the Arbitrary Body program was consistently poor. The curves of C_{n_β} are in error in slope and magnitude for all configurations and in sign at high angles-of-attack for configuration C. The predictions for C_{l_β} are optimistic, showing all three vehicles to have satisfactory positive dihedral effect ($-C_{l_\beta}$) whereas the experimental data show only configuration C to be satisfactory. If the variations in local dynamic pressure due to the bow and canopy shocks, the shadowing of the upper vertical tail surfaces at angles-of-attack, and component interference were known, and if they could be calculated by the program, then improved accuracy could be expected. It may be concluded that accurate predictions of C_{n_β} and C_{l_β} cannot be expected from the Gentry Hypersonic Arbitrary Body Program or from any other known method.

Mach Number Effects

Minimum Drag and Lift-to-Drag Ratio

One of the major design problems of any aircraft is the performance over the flight Mach number range, illustrated in Fig. 14, which shows the variation of the minimum drag coefficient and the maximum lift-to-drag ratio with Mach number for the three study concepts, A, B, and C. These data

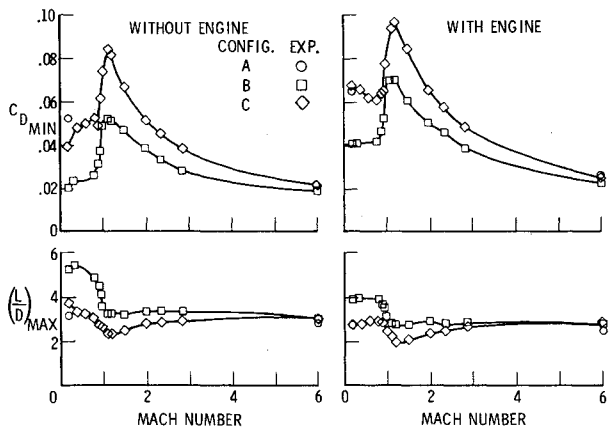

Fig. 14 Variation of $C_{D\min}$ and $(L/D)_{max}$ with Mach number.

have not been corrected to flight Reynolds numbers; however, since the tests were made at similar wind tunnel conditions, the results are considered comparable. None of the configurations have as high an $(L/D)_{max}$ as desired, particularly at subsonic landing speeds and with the engine installed. Configuration C has excessive drag compared to the other concepts, partly because it had the largest toed-in vertical tails, the largest wetted area, and the greatest nozzle expansion angle. Each of the model scramjet engines tested has been shown by trajectory analysis to be too small to provide cruise thrust at Mach 6, and an increase in engine size will further degrade the performance. The variable geometry options discussed previously are one of several ways presently under study to decrease drag and improve performance. The high drag rise through the transonic and low supersonic speed range may make area ruling a worthwhile option since no concerted effort has been made in this area.

Longitudinal Stability

Good flight characteristics are paramount for the research airplane with its widely varying flight profile. One of the characteristics of a good flying airplane is distinguished by the level of longitudinal stability it possesses throughout its design angle-of-attack and speed range. The variation of the longitudinal aerodynamic center (static margin) with Mach number is presented in Fig. 15 for the untrimmed study configurations A, B, and C, both with and without scramjet engine and at both $C_L = 0$ and 0.2. All three concepts exhibit a high level of static longitudinal stability at speeds up to $M = 3$ and satisfactory stability at $M = 6$. Since the mean aerodynamic chord of the present models is approximately one-half of the fuselage length, a static margin of 2% fuselage length would translate into 4% mean aerodynamic chord. The large static margins at off-design speeds were a consequence of the design, i.e., to maintain positive longitudinal stability up to $M = 6$. This excessive stability results in large elevon control forces to trim and leads to excessive trim drag. Even with large elevons the longitudinal control power of concept B was low.[20] Also shown are theoretical estimates of the static margin for the concepts without engine from the theories described previously for the subsonic and hypersonic speed regions and by linear theory of Ref. 21 for the $M = 1.5$ to 3.0 range. Neither the vortex lattice[12] estimates nor the theory[21] include the effects of the vertical tails which produce small increments in nose up or positive pitching moments due to their drag. The prediction at low speeds are best at $C_L = 0.2$, those at supersonic speeds by $C_L = 0$, and those at hypersonic speeds are about equal at either C_L. It may be concluded for this class of aircraft that, with the possible exception of the Gentry Program in the hypersonic speed range, the available theories give less than adequate prediction of the static margin for any purpose other than the most preliminary analysis.

Directional Stability and Dihedral Effects

Of primary importance to the safe flight of an aircraft is that the static directional stability (weather vane effect), and the dihedral effect, roll due to yaw, be positive throughout its mission. Positive directional stability and dihedral effect in coefficient form consist of $+C_{n_\beta}$ and $-C_{l_\beta}$, respectively. These parameters are presented at $C_L = 0$ as a function of Mach number in Fig. 16 for the three study concepts with and without the scramjet engine. This figure shows all configurations to have satisfactory characteristics through subsonic and supersonic speeds but only model C is satisfactory at the cruise Mach number of 6.0. The high degree of stability exhibited by model C was previously discussed in regard to its associated high drag. A prescribed level of static directional stability for models A and B at $M = 6$ could be easily obtained by use of the variable geometry flared vertical tails previously discussed on Fig. 10. The trends with Mach number at $C_L = 0.2$ were similar to those shown at $C_L = 0$ except that the experiments show an improvement in

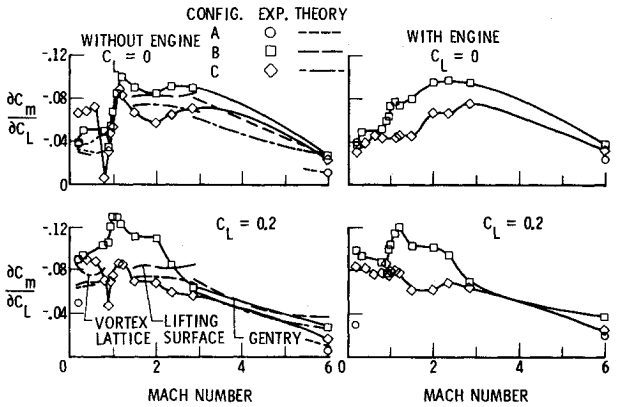

Fig. 15 Variation of longitudinal aerodynamic center with Mach number.

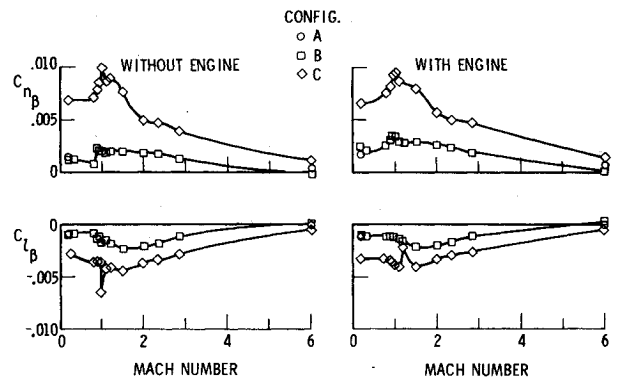

Fig. 16 Variation of directional stability and dihedral effect with Mach number.

the dihedral effect and a decrement in directional stability for each study concept. Due to the preliminary nature of the present concepts the inertial characteristics about the reference axes are unknown and therefore no comments can be made concerning the static directional stability under dynamic conditions ($C_{n_{\dot\beta}}$ dynamic).

Roll Control

Roll control was achieved by the differential deflection of the elevons for the study configurations. The results of tests across the speed range are presented in Fig. 17 for $C_L = 0$ and 0.2. These preliminary tests were conducted on the complete model configurations with scramjet engines and for zero elevon deflection. Positive values of $C_{l_{\delta h}}$ (roll due to roll control) are normal and indicate good effectiveness which is needed at all speeds and particularly at the high angles-of-attack required for pullup during transonic acceleration and during the landing maneuver. A small amount of positive $C_{n_{\delta h}}$ (yaw due to roll control) indicates good response and favorable yaw. It is not known, at this time, if the level of $C_{n_{\delta h}}$ shown for configurations A, B, and C at low Mach numbers is excessive or if the negative values of $C_{n_{\delta h}}$ for configurations A and B at $C_L = 0$ and for configurations A, B, and C at $C_L = 0.2$, present a problem. Only with simulator tests, using experimental data, accurate full-scale vehicle inertia characteristics, and a pilot in the loop could these problems be answered accurately. It may be concluded from these tests that roll control is adequate throughout the speed range but that the yaw due to roll control may be excessive at low speeds. Also, yaw due to roll control was unfavorable for models A and B at low speeds and for all models at the higher lift coefficients and Mach numbers.

Yaw Control

Yaw control is primarily required to maintain a desired heading and to implement coordinated turns. The results of

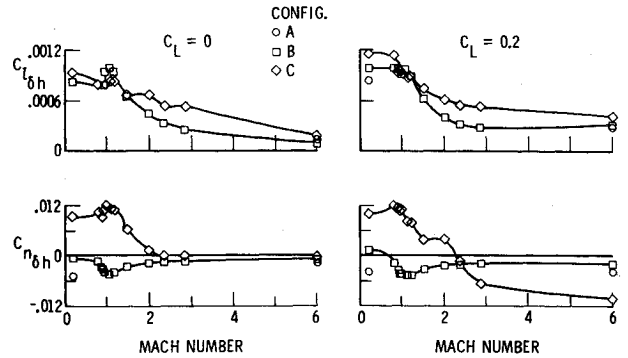

Fig. 17 Variation of roll control with Mach number, complete configuration with engine.

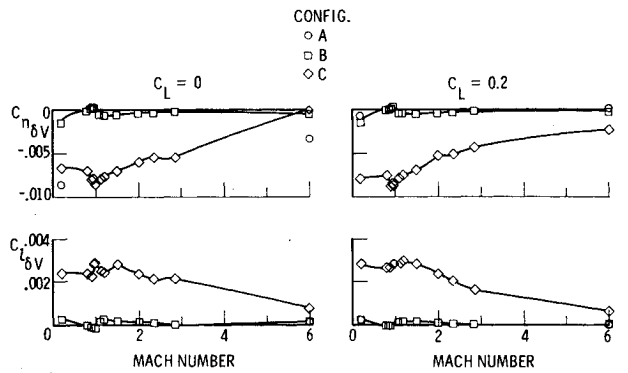

Fig. 18 Variation of yaw control with Mach number, complete configuration with engine.

tests through the Mach number range to determine the yaw control on the complete study configurations with scramjet engine are shown in Fig. 18 for both $C_L = 0$ and 0.2. None of the study configurations had adequate yaw due to yaw control ($C_{n_{\delta V}}$) under all conditions. Concept A showed good yaw control at $C_L = 0$ but no control at $C_L = 0.2$; concept B showed a small degree of yaw control at $C_L = 0$ and 0.2, and concept C showed good yaw control throughout the Mach number range except at $C_L = 0$ and $M = 6$ where the control decreased to zero. At hypersonic speeds, additional yaw control could be made available by variable geometry as previously discussed. Small positive values of roll due to yaw control ($C_{l_{\delta V}}$) are acceptable but concept C exhibits considerable roll due to yaw control ($C_{l_{\delta V}}$) throughout the Mach number range and at both $C_L = 0$ and 0.2. This excess roll due to yaw control presents a similar potential problem to that presented in the section entitled Roll Control where the yaw due to roll control was excessive. Again simulator studies are required. Concepts A and B showed negligible roll due to yaw control. It may be concluded that additional parametric tests are required to better design for yaw due to yaw control and to minimize roll due to roll control.

Concluding Remarks

An analysis of experimental data at Mach numbers of 0.2 to 6.0 on three high-volume hypersonic research airplane concepts, designed to conform to the geometry constraints of B-52 launch aircraft, indicates that all concepts were feasible but were deficient in lift and had excessive drag, particularly at subsonic landing speeds as well as a sharp drag rise at the transonic speeds. The subsonic scramjet engine drag approached that of a flat plate normal to the flow, and appears to be constant with Reynolds number. The highly swept low-aspect-ratio wings common to concepts of this type fall into a region of possible longitudinal instability. The variable geometry airfoil may be configured as a wedge or with a flared trailing edge at high Mach numbers to increase the directional stability if used on the vertical tail or to increase

the longitudinal stability if used on the elevons. Either the flared vertical tail or the flared elevon is ideally suited for use as drag brakes across the speed range. Roll control was adequate but yaw due to roll control may be a potential problem. Yaw control was inconsistent between test configurations, and ways are needed to minimize roll due to yaw control.

The vortex lattice theory gave good predictions of lift, drag due to lift, and pitching moment at subsonic speed. Current methods of drag prediction at zero lift are undependable, as are predictions of trim and static margin, and therefore wind tunnel measurements must be relied upon. Predictions of longitudinal stability at supersonic Mach numbers were good. The Gentry Hypersonic Arbitrary Body Program gave good predictions of the trends, including the local slopes of lift, drag, and pitching moment with angle-of-attack. The level of the values, however, of pitching moment, drag, and lift-to-drag ratio and the angle-of-attack for zero lift and pitching moment were not consistently predicted. No currently available theory or program gives accurate predictions of directional stability or dihedral effects at hypersonic speeds. Wind tunnel tests must again be relied upon to supplement prediction methods.

References

[1] Hearth, D.P. and Preyss, A.E., "Hypersonic Technology—Approach to an Expanded Program," *Astronautics and Aeronautics,* Vol. 14, Dec. 1976, pp. 20–37.

[2] Braslow, A.L. and Knox, E.C., "Simplified Method for Determination of Critical Height of Disturbed Roughness Particles for Boundary-Layer Transition at Mach Numbers from 0 to 5," NACA TN 4363, 1958.

[3] Armstrong, N.A. and Matranga, G.J., "Approach and Landing Investigation at Lift-Drag Ratios of 2 to 4 Utilizing a Straight-Wing Fighter Airplane," NASA TM X-31, Aug. 1959.

[4] Combs, H.G. et al., "Configuration Development Study of the X-24C Hypersonic Research Airplane," NASA CR-145032, Dec. 1976; NASA CR-145074, Jan. 1977; and NASA CR-145103, Jan. 1977.

[5] Creel, T.R. Jr. and Penland, J.A., "Low Speed Aerodynamic Characteristics of a Hypersonic Research Airplane Concept Having a 70° Swept Delta Wing," NASA TM X-71974, 1974.

[6] Penland, J.A., Fournier, R.H., and Marcum, D.C. Jr., "Aerodynamic Characteristics of a Hypersonic Research Airplane Concept Having a 70° Swept Double-Delta Wing at Mach Numbers from 1.50 to 2.86," NASA TN D-8065, 1975.

[7] Henry, J.R. and Anderson, G.Y., "Design Considerations for the Airframe-Integrated Scramjet," NASA TM X-2895, Dec. 1973.

[8] Weidner, J.P., Small, W.J., and Penland, J.A., "Scramjet Integration on Hypersonic Research Airplane Concepts," *Journal of Aircraft,* Vol. 14, May 1977, pp. 460–466.

[9] Johnston, P.J., Pittman, J.L., and Huffman, J.K., "Effect of an Integrated Scramjet Installation on the Subsonic Performance of an Aircraft Designed for Mach 6 Cruise," *Journal of Aircraft,* Vol. 15, June 1978, pp. 326–332.

[10] Spreemann, K.P., "Design Guide for Pitch-up Evaluation and Investigation at High Subsonic Speeds of Possible Limitations Due to Wing-Aspect-Ratio Variations," NASA TM X-28, Aug. 1959.

[11] Penland, J.A., Creel, T.R. Jr., and Howard, F.G., "Experimental Low-Speed and Calculated High-Speed Aerodynamic Characteristics of a Hypersonic Research Airplane Concept Having a 65° Swept Delta Wing," NASA TN D-7633, 1974.

[12] Lamar, J.E. and Gloss, B.B., "Subsonic Aerodynamic Characteristics of Interacting Lifting Surfaces with Separated Flow Around Sharp Edges Predicted by a Vortex-Lattice Method," NASA TN D-7921, 1975.

[13] Polhamus, E.C., "A Concept of the Vortex Lift of Sharp-Edge Delta Wings Based on a Leading-Edge-Suction Analogy," NASA TN D-3767, 1966.

[14] Pittman, J.L. and Dillon, J.L., "Vortex Lattice Prediction of Subsonic Aerodynamics of Hypersonic Vehicle Concepts," *Journal of Aircraft,* Vol. 14, Oct. 1977, pp. 1017–1019.

[15] Hoerner, S.F., *Fluid-Dynamic Drag,* Hoerner Fluid Dynamics, Brick Town, N.J., 1958.

[16] McLellan, C.H., "A Method for Increasing the Effectiveness of Stabilizing Surfaces at High Supersonic Mach Numbers," NACA RM L54F21, Aug. 1954.

[17] Gellert, G.O., "Geometric Computing—Electronic Geometry for Semiautomated Design," *Machine Design,* Vol. 37: "Part 1: The Method and Its Application," March 18, 1965, pp. 152–159; "Part 2: Fields of Application," April 1, 1965, pp. 94–100.

[18] Gentry, A.E., "Hypersonic Arbitrary-Body Aerodynamic Computer Program (Mark III Version)," Rept. DAC 61552, Vols. I and II, Apr. 1968.

[19] Stack, S.H., Edwards, C.L.W., and Small, W.J., "GEMPAK: An Arbitrary Aircraft Geometry Generator," NASA TP-1022, Oct. 1977.

[20] Dillon, J.L. and Pittman, J.L., "Aerodynamic Characteristics at Mach Numbers from 0.33 to 1.20 of a Wing-Body Concept for a Hypersonic Research Airplane," NASA TP-1044, Dec. 1977.

[21] Middleton, W.D. and Carlson, H.W., "Numerical Method of Estimating and Optimizing Supersonic Aerodynamic Characteristics of Arbitrary Planform Wings," *Journal of Aircraft,* Vol. 2, July–Aug. 1965, pp. 261–265.